

JOURNAL of CIVIL ENGINEERING and MANAGEMENT

2025 Volume 31 Issue 8 Pages 843–859

https://doi.org/10.3846/jcem.2025.24061

COLLABORATIVE ANALYSIS MODEL OF CONSTRUCTION SCHEDULE AND QUALITY FOR RCC DAM BASED ON DES AND DEEP LEARNING

Geng ZHANG, Binping WU, Bingyu REN[™], Tao GUAN, Jia YU

State Key Laboratory of Hydraulic Engineering Intelligent Construction and Operation, Tianjin University, 135 Yaquan Road, Jinnnan District, Tianjin 300350, China

Article History:

- received 22 October 2024
- accepted 17 February 2025

Abstract. Construction schedule simulation is an effective method to analyze the progress of concrete rolling construction and its simulation accuracy is an important indicator that project managers care about. However, existing roller compacter concrete construction simulation research pays less attention to the impact of construction process changes caused by compaction quality on simulation accuracy. Based on the real-time monitoring system of concrete rolling construction, this paper establishes a simulation model of concrete rolling construction considering compaction quality. The model firstly reconstructs the property parameters of roller compacted concrete using the improved generated adversarial network, secondly, considering the nonlinear correlation characteristics of parameters affecting compaction quality, a concrete compaction quality analysis model based on improving grey wolf optimized convolutional neural networks (IGWO-CNN) was built. Finally, the intelligent analysis model of compaction quality was embedded into the simulation model of concrete rolling construction. Based on real-time monitoring data, the simulation model was driven and the simulation process was adjusted adaptively. Taking the construction of a roller compacted concrete dam in China as an example, the validity and superiority of this model are proved.

Keywords: construction simulation, concrete rolling construction, real-time monitoring, compaction quality, improved generative adversarial networks, improving grey wolf optimized convolutional neural networks.

1. Introduction

Roller Compacted Concrete (RCC) is a specialized type of concrete widely used in heavy construction, particularly for large-scale infrastructure projects such as dams (Liu et al., 2015a), roads (Aghaeipour & Madhkhan 2020), airports (Zhang et al., 2022), and navigation-power junction project (Zhang & Zeng, 2018). It is named for the construction method used, where the concrete is compacted using rollers rather than being poured and vibrated like conventional concrete. RCC has become a preferred material for large infrastructure projects due to its durability, speed of construction, and cost-efficiency. Roller compaction is a crucial stage in the concrete construction process and is one of the key factors in ensuring construction quality and project schedule. Therefore, in RCC dam construction, roller compaction is highly valued by project managers.

In order to achieve effective construction schedule control, researchers have investigated many construction simulation methods. Halpin (1977) proposed a discrete event simulation method called CYCLONE for repetitive projects. After that simulation methods like UM-CYCLONE

(Ioannou, 1990), MODSIM (Oloufa, 1993), STROBOSCOPE (Martinez & Ioannou, 1994), Simphony (AbouRizk & Mohammed, 2000), SDESA (Lu, 2003) have been proposed. These methods bridge the gap between the real construction system and the abstract simulation model, facilitating the wide use of construction simulation in today's construction management. In 2010, Dynamic-Data-Driven Application Systems' comprehensive system architecture and methodology (Celik et al., 2010) were proposed. For look-ahead planning during field activities, a dynamic real-time monitoring and simulation of heavy construction operations (Song & Eldin, 2012) was offered. In order to constantly improve the simulation model, an overarching tracking-technology-independent architecture (Vahdatikhaki & Hammad, 2014) based on the incorporation of new location tracking technologies was developed. In tunnel case study, Zhang et al. (2014) adopted a Bayesian technique to continuously update duration distributions of uncompleted construction activities based on onsite data. Akhavian and Behzadan (2015) gathered real da-

[™]Corresponding author. E-mail: renby@tju.edu.cn

ta from construction equipment, and then utilized a machine learning technique for simulation. In 2016, a rockfill dam construction simulation model (Du et al., 2016) based on flow shop construction was presented. In order to design snow removal projects while taking weather and truck-related data gathered by real-time sensors into consideration, Mohamed et al. (2017) suggested a data-driven simulation framework. In addition to schedule, Ji and AbouRizk (2018) established a data-driven simulation model to aid decision support systems in estimating and controlling the costs of quality-induced rework in the production of building products. As artificial intelligence advances, many artificial intelligence algorithms are used in simulation models, such as evolutionary method inspired by chaos theory (Shrestha & Behzadan, 2018), fuzzy Bayesian update algorithm (Guan et al., 2018), Bayesian field theory (Zhang et al., 2020), improved extreme gradient boosting (XGBoost) approach (Lv et al., 2020), optimized hybrid-kernel RVM (Song et al., 2020), enhanced semi-supervised ensemble machine learning approach (Zhang et al., 2023).

These simulation models provide a good theoretical basis for the simulation of concrete rolling construction. Above all, discrete event simulation method is an important means of analyzing the progress of concrete rolling construction (Hu et al., 2019a). Concrete rolling construction simulation (Zhong et al., 2015) is the key of construction management, which can avoid reworks and operation conflictions, improve the resource utilization rate and save project time and cost. Wang et al. (1995) used system simulation and a queue stochastic simulation network to simulate roller compacted concrete dam construction. Luo et al. (2009) proposed a petri net based simulation method to analyze the interaction relationship between the roller compacted concrete dam production, transportation and placement process. Zhao et al. (2013) studied the roller compacted concrete pouring process system and construction schedule optimization for the limited resource conditions of roller compacted concrete dams. Wang et al. (2018b) proposed an RCC dam construction simulation approach that uses Bayesian updating method and real-time monitoring technology to update the simulation model. Hu et al. (2019b) used the DPM model to analyze the perception data, determines the probability density distribution of the simulation parameters, and uses the SUGS algorithm improved by permutation entropy to quickly solve the DPM model under the real-time perception data stream, so as to realize the adaptive update of the simulation parameters.

However, through a literature review, it was found that most of the current articles on RCC dam construction simulation primarily focus on updating simulation parameters and do not consider the impact of compaction quality on the construction schedule of RCC dams. Compaction quality of roller compacted concrete, a significant index of rolling process simulation model, has significant impact to the construction simulation results. The reason is that it

can determine whether additional compaction of the surface is needed and whether the simulation logic needs to be adjusted. Therefore, the paper developed an algorithm to more accurately assess the compaction quality, which can not only finely analyze the construction quality of the storehouse surface, but also improve the accuracy of the schedule simulation.

Construction quality of rolling process is another concern of project managers (Liu et al., 2015a; Zhong et al., 2017). Many scholars have carried out research on the quality control of different construction materials in the rolling process, such as earth-rock material (Liu et al., 2012) and asphalt (Hu et al., 2019a). As for compaction quality of roller compacted concrete, based on the integration of global navigation satellite system (GNSS) techniques, network transmission technology and sensor technology, Liu et al. (2015b) proposed a real-time construction quality monitoring model for storehouse surfaces of RCC dams, built a real-time construction quality monitoring system. The digital monitoring of roller compaction quality has realized the parameters of storehouse surface roller compaction (rolling trajectory of roller compaction machine, walking speed, number of roller compaction, excitation force, etc.) all-weather and real-time monitoring. At the same time, in order to realize the analysis of compaction quality, mathematical statistical methods and artificial intelligence methods have been successively applied to evaluating compaction quality. Statistical methods mainly include linear regression, etc. Artificial intelligence methods (Wang et al., 2018a; Hong et al., 2020) include artificial neural network methods, support vector machine methods, and deep learning-based methods, etc.

Compared with statistical methods, artificial intelligence-based methods can effectively deal with non-linear relationships in data. In recent years, due to the outstanding ability of deep learning algorithms to process nonlinear mapping, they have gradually been used in the field of prediction. Convolutional neural network (CNN) is one of the most popular architectures in deep learning. It shows great potential and innovative achievements in solving regression problems, such as probabilistic wind power forecasting (Wang et al., 2017), NIR calibration (Cui & Fearn, 2018) and spatial prediction of groundwater potential mapping (Panahi et al., 2020). Meanwhile, in order to improve the ability of neural networks to solve problems in various fields, the application of evolutionary computing to optimize neural networks has made great progress (Baldominos et al., 2020; Xu et al., 2022). In this paper, an improved gray wolf optimization algorithm is used to optimize a one-dimensional convolutional neural network to improve its compaction quality prediction performance.

2. Research objective and contributions

Related research has achieved rich results in the construction simulation of roller compacted concrete and real-time monitoring of the roller compacted construction process. However, the existing concrete rolling construction simulation model does not consider the adjustment of the simulation process brought about by the dynamic changes of the rolling quality of the construction site. In the existing simulation model of concrete rolling construction, the sequence of activity nodes consisting of unloading, paving, rolling and quality inspection is statically fixed, and the simulation process composed of process activity nodes in a fixed sequence reflects the ideal process. In fact, in actual concrete rolling construction, supplementary rolling activity will happen according to the construction quality, which means that the actual sequence of activities is dynamically adjusted.

In this paper, aiming at solving above problems, a simulation method for roller compacted concrete placement process is proposed. Firstly, in order to enhance the authenticity of the simulation model and improve the simulation accuracy, this paper is based on the concrete rolling construction digital monitoring system (Liu et al., 2015b) to obtain rolling parameters and concrete property parameters, and at the same time use the improved generative adversarial networks (IGAN) to reconstruct the concrete property monitoring data to solve the problem of the small number of samples caused by the long collection time interval. The main improvement idea of this paper is firstly using Long Short Term Memory (LSTM) neurons in the Generator. After each LSTM layer, a batch normalization layer is added to improve the network training speed. Secondly, to achieve accurate analysis of compaction quality, this paper use improving grey wolf optimized convolutional neural networks establish an intelligent analysis model of compaction degree, and obtain a high-precision compaction quality analysis model through the training of on-site measured compaction data, so as to realize precise analysis of the degree of compaction at any position of the storehouse surface during the simulation process. Finally, the quality intelligent analysis model is embedded in the concrete rolling construction simulation model, and the simulation process is updated in real time based on the quality analysis results.

3. Research framework

The overall research framework of simulation model of roller compacted concrete construction is shown in Figure 1

4. Methodology of construction simulation model considering quality factors

The mathematical model of concrete rolling construction simulation is composed of four parts: objective function, state transition equation, simulation parameters, simulation constraints.

(1) Objective function:

$$T = f(Q_R(c,r), M_c, M_{q_s}, S, C).$$
(1)

In Eqn (1), T is the storehouse's simulation duration, $f(\cdot)$ is simulation solution function, $Q_R(c,r)$ is compaction quality, meanwhile, c is concrete property parameters, r is rolling parameters. M_c is the set of construction technology, including horizontal layer construction and slopping layer construction. M_q is the set of compaction quality analysis method. S is the set of construction monitoring parameter. C is the construction condition.

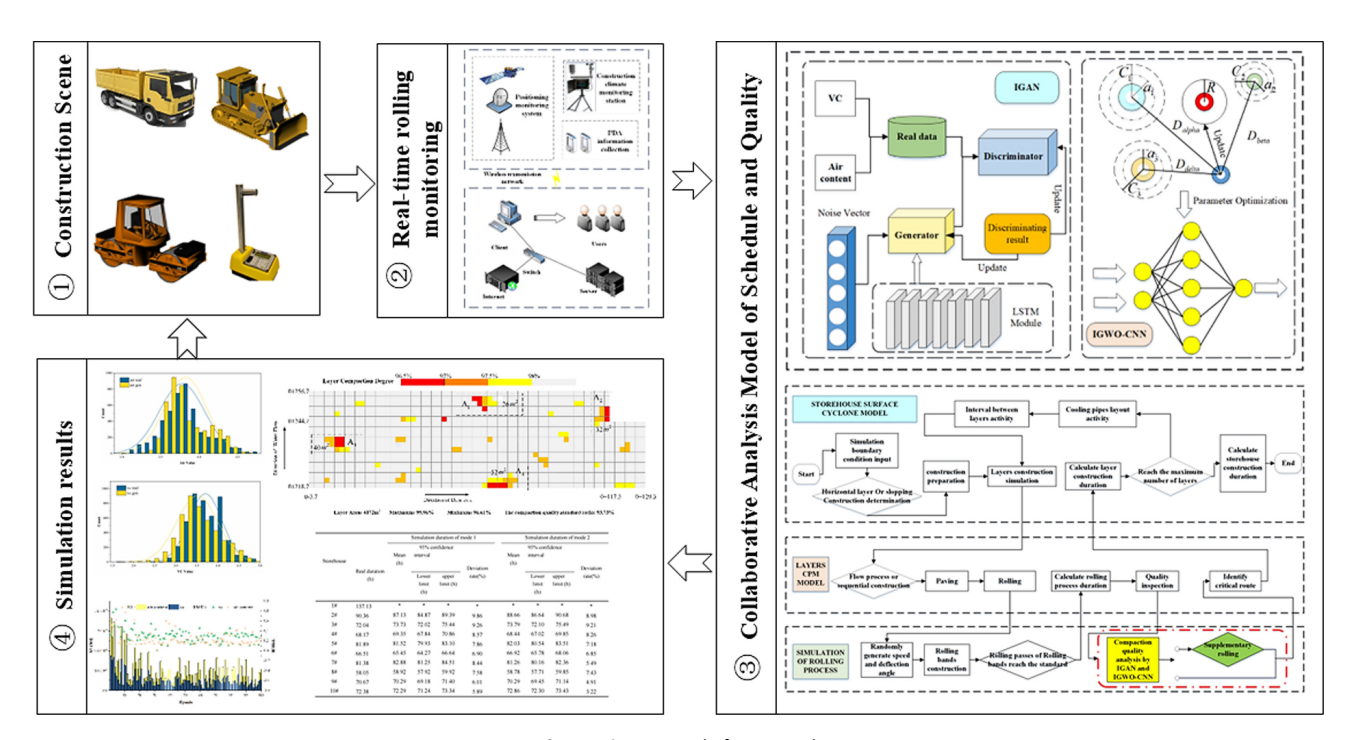


Figure 1. Research framework

(2) State transition equation:

$$\begin{cases} T_{(S,i)} = T_{(S,i-1)} + \Delta t \\ T_{(L,i)} = T_{(L,i-1)} + \Delta t \\ T_{(r,i)} = T_{(r,i-1)} + \Delta t \\ H(S,i) = H(S,i-1) + n_L(\Delta t) * h_L \\ N_{(L,i)} = N_{(L,i-1)} + n_L(\Delta t) \\ N_{(r,i)} = N_{(r,i-1)} + n_r(\Delta t) \\ x_i = x_{i-1} + v_{t-1} \Delta t \cos \theta_{t-1} \\ y_i = y_{i-1} + v_{t-1} \Delta t \sin \theta_{t-1} \end{cases}$$

$$(2)$$

During the simulation, Eqn (2) specifies the state transfer function. $T_{(S,i)}$ represents the storehouse surface construction duration at simulation moment t_i , $T_{(L,i)}$ represents the layer construction duration at simulation moment t_i , $T_{(r,i)}$ represents the rolling construction duration at simulation moment t_i , Δt is the simulation clock step length, H(S,i) represents the storehouse surface height at simulation moment t_i , $n_L(\Delta t)$ is the number of layers poured in Δt , h_L is layer thickness, $N_{(L,i)}$ indicates the serial number of layer, $N_{(r,i)}$ is the serial number of rolling band, $n_r(\Delta t)$ is the number of rolling band poured in Δt , x_i and y_i represent the coordinates of the roller at simulation moment t_{i-1} , θ_{t-1} is the roller instantaneous deflection angle at simulation moment t_{i-1} .

(3) Simulation parameters:

$$\begin{aligned} Q_R &= \left[v_{\text{inf}}, \ v_{\text{sup}}, \Delta V_{vc}, \Delta V_{ac}, \ N_1, N_2 \right]; \\ M_c &= M_c \left(P \right) \cup M_c \left(X \right); \\ M_q &= M_q \left(R \right) \cup M_q \left(E \right); \\ S &= \left[v, \theta, N_1, N_2, V_{vc}, V_{ac} \right]; \\ C &= \left[A, N \right]. \end{aligned} \tag{3}$$

Equation (3) gives the set of simulation parameters. $v_{\rm inf}$ and $v_{\rm sup}$ are rolling speed boundary. ΔV_{vc} and ΔV_{ac} represent the change value of vc and air content respectively. $M_c(P)$ is horizontal layer construction, $M_c(X)$ slopping layer construction. $M_q(R)$ is concrete property parameters reconstruction method, $M_q(E)$ is construction quality evaluation method. v is the roller speed, θ is the roller instantaneous deflection angle, N_1 represents the number of static rolling passes, N_2 represents the number of vibration rolling passes, V_{vc} is defined as the value of VC, V_{ac} is defined as the value of air content. A is the construction storehouse surface boundary, N is the number of construction machinery.

(4) Simulation constraints:

$$\begin{aligned} Q_{R}(s) &\subset Q_{R}(base); \\ A &\leq A_{c}; \ N \leq N_{c}; \\ q_{s} &\leq q_{N}; \\ T_{e}(L,j) - T_{s}(L,j-1) &\leq T_{0}. \end{aligned} \tag{4}$$

Equation (4) is the simulation constraints. $Q_R(s)$ is the compaction quality calculated in simulation, $Q_R(base)$ is Construction specification requirements according to "Construction Specifications for Hydraulic RCC (DL/T5112-2009)" (National Energy Administration of People's Republic of China, 2009). And it is also required that the storehouse surface boundary A in the construction simulation should not exceed the storehouse surface range A_c which was inputted before the simulation begins, the number of construction machinery N cannot exceed the specified number of construction machinery N_c , q_s is the standard ratio of the rolling area in layer. q_N is layer compaction quality standard ratio in simulation. $T_s(L, j-1)$ is the start time of layer j - 1, $T_{\rho}(L, j)$ the rolling activity end time of layer j. T_0 denotes the allowed construction time interval between adjacent layers.

4.1. Simulation parameters determination

4.1.1. Rolling parameters

(1) Calculation of rolling passes

As shown in the Figure 2, the concrete rolling construction is a random walking process of the roller under the combined action of rolling speed and deflection angle.

The calculation diagram of the number of rolling passes under different vibration conditions is shown in the Figure 3.

The roller width is assumed to be L cm, and the store-house surface is gridded to calculate the rolling passes under different vibration states. At the same time, the number and coordinates of each grid are obtained. Let the point coordinates of the roller at simulation moment t_{i-1}

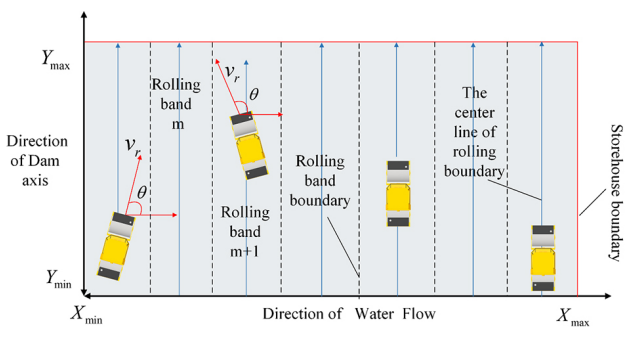


Figure 2. Diagram of rolling process

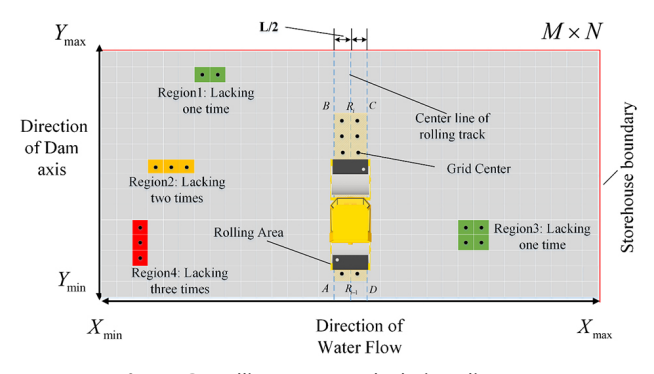


Figure 3. Rolling passes calculation diagram

and t_i be $R_{i-1}(x_{i-1}, y_{i-1})$ and $R_i(x_i, y_i)$ respectively. Determine the rolling area A_r within the time interval Δt , A_r is a quadrilateral region where line $R_{i-1}R_i$ extends L/2 in the vertical direction of the roller trajectory line. Let the coordinates of the four vertices of A_r be $P_A(x_A, y_A)$, $P_B(x_B, y_B)$, $P_C(x_C, y_C)$, $P_D(x_D, y_D)$. The Bresenham algorithm was used for determining grid-based rolling areas due to its efficiency in rasterizing linear paths with integer arithmetic. Specifically, the algorithm is employed to map the roller's path onto a discrete grid by identifying the sequence of grid cells traversed during each compaction pass. This ensures efficient rasterization of the roller's coverage area while minimizing computational complexity due to the integerbased calculations inherent in the Bresenham approach. According to Bresenham Algorithm (Flangan, 1990), the coordinate relationship between points ABCD and points $R_{i-1}(x_{i-1}, y_{i-1}), R_i(x_i, y_i)$ satisfies the following formula:

$$\sqrt{(x_{i-1} - x_A)^2 + (y_{i-1} - y_A)^2} = \frac{L}{2};$$

$$\left[\frac{x_{i-1} - x_A}{y_{i-1} - y_A}\right] \times \left[\frac{x_{i-1} - x_i}{y_{i-1} - y_i}\right] = -1;$$

$$\sqrt{(x_i - x_B)^2 + (y_i - y_B)^2} = \frac{L}{2};$$

$$\left[\frac{x_i - x_B}{y_i - y_B}\right] \times \left[\frac{x_{i-1} - x_i}{y_{i-1} - y_i}\right] = -1;$$

$$\sqrt{(x_i - x_c)^2 + (y_i - y_c)^2} = \frac{L}{2};$$

$$\left[\frac{x_i - x_c}{y_i - y_c}\right] \times \left[\frac{x_{i-1} - x_i}{y_{i-1} - y_i}\right] = -1;$$

$$\sqrt{(x_{i-1} - x_D)^2 + (y_{i-1} - y_D)^2} = \frac{L}{2};$$

$$\left[(x_{i-1} - x_D)/(y_{i-1} - y_D)\right] \times \left[(x_{i-1} - x_i)/(y_{i-1} - y_i)\right] = -1.$$

According to the divided grid, determine which grid center is in this area A_n , if the center point of the grid is located in area A_n , then the grid increases the number of rolling passes under the corresponding vibration state.

(2) Rolling speed determination

Based on the real-time monitoring system of the rolling construction process, the probability density distribution of the rolling speed is obtained.

4.1.2. Concrete property parameters

According to "Construction Specifications for Hydraulic RCC (DL/T5112-2009)" (National Energy Administration of People's Republic of China, 2009), the frequency of detection of VC value is once every 2 h, and the frequency of detection of gas content is once per shift. The number of samples is not enough for the simulation parameters. Therefore, this paper uses the improved generation adversarial networks to expand the number of concrete property parameter monitoring data samples, and provides sufficient simulation parameters for the simulation of the roller compacted concrete construction to improve the simulation accuracy. GAN is a generative model proposed by

Goodfellow in 2014. GAN has been widely used in the field of image and computer vision. At the same time, GAN is also widely used in data augmentation and scenario generation and missing values imputation (Chen et al., 2018; Zhang et al., 2021). It consists of a generator and a discriminator (Goodfellow et al., 2014). Based on the literature (Gulrajani et al., 2017), this paper considers the time series characteristics of concrete property parameter monitoring data, and introduces LSTM into the generator to improve the reconstruction effect.

Improved the generative adversarial networks to reconstruct the VC value and data of the air content sample, and then use the probability density estimation method based on the DPM model to determine the parameter probability density distribution.

Select the completed roller compacted concrete property parameter data of the storehouse surface in the realtime monitoring system as the training set, select *i* groups data of concrete storehouse surfaces in the real-time monitoring system, and the monitoring data is defined as x_i . Due to the intricate distribution relationship between realtime monitoring data such as VC and air content, suppose it is $p_r(x)$, $p_r(x)$ is difficult to describe through explicit mathematical model. Suppose there is a set of noise vectors that obey the joint Gaussian distribution $p_{z}(z)$. At the same time, a deep neural network with the ability to handle complex nonlinearities is used to establish the mapping relationship between $p_z(z)$ and $p_r(x)$. As a result, by sampling from a known distribution as input, new data that satisfies the distribution relationship of original data can be generated.

The establishment process of the mapping is realized through the training of GAN, the basic structure of GAN network is shown in the Figure 4. GAN consists of two parts: generator $G(\theta^{(G)})$ and discriminator $G(\theta^{(D)})$, where $\theta^{(G)}$ and $\theta^{(D)}$ respectively represent the weights of the two networks.

As a generator $G(\theta^{(G)})$ gets random vectors from some prior noise distribution. In an attempt to confuse $G(\theta^{(D)})$ into giving false discriminative results, the generator transforms these vectors into a distribution as close as possible to the real sample data. In our research, we aimed to en-

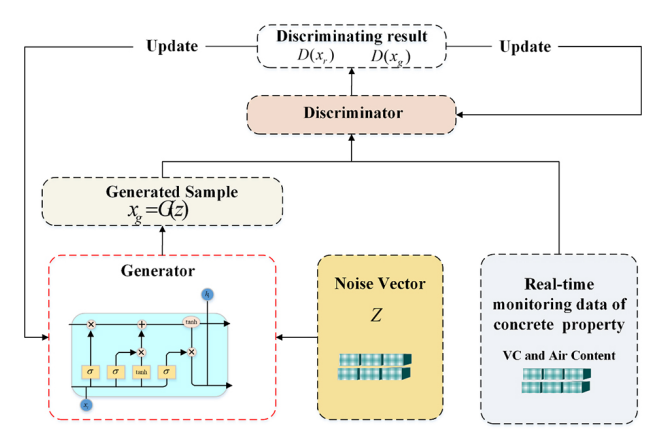


Figure 4. Concrete property monitoring data reconstruction framework based on IGAN

hance the performance of traditional GANs by addressing some of their inherent limitations. The introduction of LSTM layers allows our model to better capture long-term dependencies in the data, which is particularly beneficial for sequences that exhibit temporal patterns. This capability is critical in generating more coherent and contextually relevant outputs, as it enables the model to maintain information over longer intervals compared to standard GAN architectures. Additionally, the incorporation of batch normalization layers serves to stabilize the learning process by normalizing the input to each layer, which helps mitigate issues such as internal covariate shift. This leads to faster convergence and improved overall performance, as it allows the model to learn more effectively from the training data. Instead, the discriminator $G(\theta^{(D)})$ attempts to judge whether an input sample is a sample obtained from real data or a synthetic sample. At the same time, for a given noise vector z, $G(\theta^{(G)})$ outputs synthetic samples $x_q = G(z)$. $G(\theta^{(D)})$ gets real sample x_r and the generated sample x_a . Then, it outputs probability values $D(x_r)$ and $D(x_a)$, which indicate whether the input samples come from real data. During the adversarial training process, the generator attempts to generate samples as close as possible to the real data distribution and makes the generated sample x_a to confuse the discriminator to give the result as $D(x_a) = 1$, while the discriminator attempts to give the result as $D(x_a) = 0$ and $D(x_r) = 1$.

The loss functions are defined as follows:

$$L_{G} = -E_{z \sim p_{z}(z)} \Big[D(G(z)) \Big];$$

$$L_{D} = -E_{x \sim p_{r}(x)} \Big[D(x) \Big] + E_{z \sim p_{z}(z)} \Big[D(G(z)) \Big].$$
(6)

In Eqn (6), E represents the expected distribution; G(z) represents the data generated by the generator, and $D(\sim)$ represents the output of the discriminator network. The training process of GAN can be regarded as a zero-sum game problem in essence. The objective function of the game process is:

$$\min_{G} \max_{D} V(G, D) = \mathbb{E}_{x \sim p_r(x)}[D(x)] - \mathbb{E}_{z \sim p_z(z)}[D(G(z))].$$
 (7)

After the adversarial training process is finished, a Nash equilibrium will be reached between $G(\theta^{(G)})$ and $G(\theta^{(D)})$. And the generator $G(\theta^{(G)})$ tends to generate samples close to the true distribution, and the discriminator $G(\theta^{(D)})$ tends to give the result that the probability of generating samples and real samples is equal. Eqn (7) ensures the generated data closely matches the real distribution, enhancing model accuracy in real-time concrete property parameters reconstruction.

The detailed network parameters of the generator are shown in Table 1.

The detailed network parameters of the discriminator are shown in Table 2.

The choice of the size of the SpectralNormalization (Conv1D) convolution kernel and the number of filters is determined by experiments.

Table 1. Generator network structure

Layer	Name	Name Parameters	
1	LSTM	units	256
		activation	tanh
		recurrent activation	sigmoid
2	Batch Normalization	momentum	0.9
3	LSTM	units	128
		activation	tanh
		recurrent activation	sigmoid
4	Batch Normalization	momentum	0.9
5	LSTM	units	64
		activation	tanh
		recurrent activation	sigmoid
6	Batch Normalization	momentum	0.9
7	concatenate	/	/
8	Dense	units	32
9	Batch Normalization	momentum	0.9
10	LeakyReLU	/	/
11	dense	units	2

Table 2. Discriminator network structure

Layer	Name	Parameters	Value
1	Spectral Normalization	filters	64
	(Conv1D)	kernel size	4
2	LeakyReLU	/	/
3	Spectral Normalization	filters	128
	(Conv1D)	kernel size	4
4	LeakyReLU	/	/
5	Dropout	rate	0.2
6	Spectral Normalization	filters	196
	(Conv1D)	kernel size	4
7	LeakyReLU	/	/
8	Dropout	rate	0.2
9	Spectral Normalization	filters	392
	(Conv1D)	kernel size	4
10	LeakyReLU	/	/
11	Flatten	/	/
12	Dense	units	32
13	LeakyReLU	/	/
14	Dropout	rate	0.15
15	concatenate	/	/
16	Dense	units	16
17	LeakyReLU	/	/
18	Dense	units	1

4.2. Construction quality analysis

The parameters affecting the compaction quality of the storehouse surface include rolling parameters and concrete property parameters. This paper uses IGWO-CNN to establish the nonlinear mapping relationship between vc, air content, rolling passes, rolling speed and compaction degree. Simultaneously, in order to improve GWO algorithm optimization performance, this paper makes the

following two improvements on the basis of the literature (Faris et al., 2018).

(1) Since the convergence factor *a* affects the global search ability and local exploration ability of the algorithm, the value of the convergence factor a in the original gray wolf algorithm decreases linearly from 2 to 0, which is easy to cause the algorithm to converge prematurely and fall into a local optimum. To solve this problem, the nonlinear cosine convergence factor is introduced as the first improvement, which can avoid the prematurity of the algorithm. The expression is:

$$a = 2\cos\left(\frac{\pi}{2} \times \frac{iter}{Max/ter}\right). \tag{8}$$

(2) When the individual gray wolf is updating the position, the traditional GWO still has defects such as easy to fall into slow convergence and local optimum. In order to further improve the performance of the algorithm and avoid the complexity of the algorithm, the Gaussian mutation operator is added to the gray wolf position update equation as the second improvement. The basic form is as follows:

$$X_{iter}' = X_{iter} \left[1 + \frac{|a|}{2} f_{\mu,\sigma^2}(x) \right];$$

Table 3. Pseudo-Code of IGWO-CNN

$$f_{\mu,\sigma^2}(x) = \frac{1}{\sigma\sqrt{2\pi}} \exp(-\frac{(x-\mu)^2}{2\sigma^2}).$$
 (9)

Due to the non-linear relationships of the real-time monitoring data of concrete construction, this paper adopts the Convolutional Neural Network Optimized by Improved Grey Wolf Optimization Algorithm (IGWO-CNN) to adaptively solve the nonlinear correlation in multivariate data. The pseudo code of the algorithm is shown in Table 3.

In this way, the accuracy and generalization ability of the evaluation of roller compacted concrete compaction quality is improved. Hyperparameter optimized using IG-WO including batch size, number of kernels, kernel size, their value ranges from [1, 20], [10, 50], and [1, 4] respectively. The CNN network structure used in this paper is shown in the Figure 5. In Figure 5, w_i and h_i represent the width and height of the input vector, respectively in input layer. c_w and c_h are the width and height of kernel size. w_c and h_c respectively represent the width and height of the feature map in the convolutional layer. In this paper, both h_i and h_c are 1.

The training process of the CNN (Goodfellow et al., 2016) network in the paper is as follows.

(1) Forward- propagation

In each layer of CNN model, the forward propagation algorithm is applied to calculate the output of each layer

Algorithm 1. The Proposed Evaluating Algorithm (IGWO-CNN)

Input: The number of population N_{pop} and the maximum number of iterations N_{iter}

Output: Compaction degree

Begin

1: Divide dataset into train set D_r and test set D_{ei}

2: Initialize the parameter a, A and C and the population of gray wolves $X_i (i = 1, 2 \cdots N_{non})$;

3: for
$$(i \leq N_{pop})$$
 do

4: Set the value of X_i as a hyperparameter for the CNN model;

5: Computing the fitness of X_i is performed using Eqn (11) for D_r and set it as the loss of CNN;

6: end for

7: Set X_{α} , X_{β} , X_{δ} as the best solution, second best solution, third best solution, respectively;

8: while
$$(n \le N_{iter})$$
 do

9: **for** each X_i **do**

10: Perform the Gaussian mutation operator by Eqn (9);

11: Update X_i position;

12: Set the value of X_i as a hyperparameter for the CNN model;

13: Computing the fitness of X_i is performed using Eqn (11) for D_r and set it as the loss of CNN;

14: end for

15: Update a using Eqn (8) A and C;

16: X_{α} , X_{β} and X_{δ} Update;

17: n = n + 1;

18: end while

19: Set the value of X_{α} as best hyperparameter for the CNN model;

20: Evaluate the compaction degree in D_e using the optimized CNN model;

End

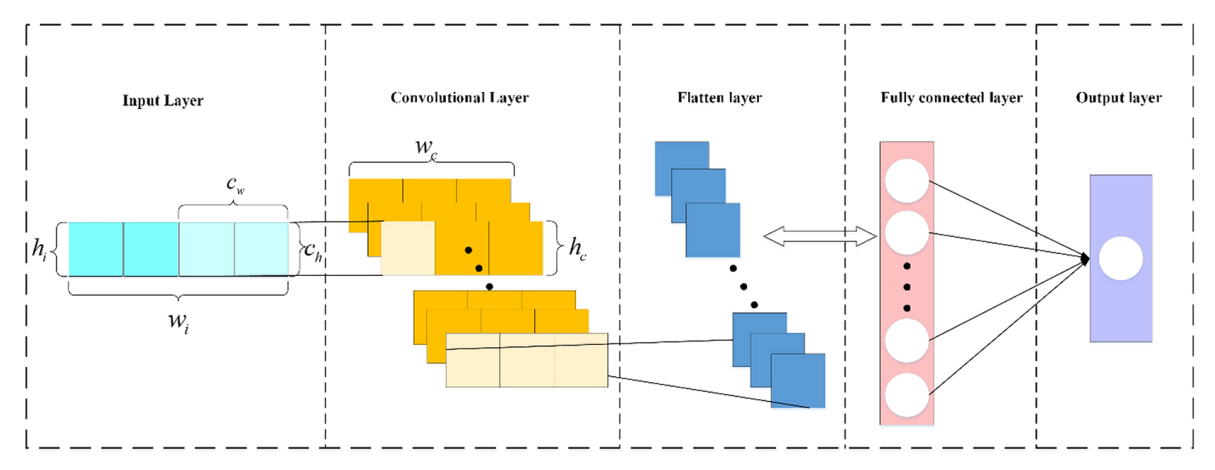


Figure 5. CNN structure in the paper

of neurons. The neuron input and output calculation formula are as follows:

$$x_{k}^{m} = b_{k}^{m} \sum_{i=1}^{m-1} conv1D(w_{ik}^{m-1}, s_{i}^{m-1});$$

$$y_{k}^{m} = f(x_{k}^{m}).$$
 (10)

In Eqn (10), the bias of kth neuron in m layer is defined as b_k^m , the weight from the ith neuron in m-1 layer to the kth neuron in m layer is defined as w_{ik}^{m-1} , the output of the ith neuron in m-1 layer is defined as s_i^{m-1} . x_k^m is the kth input in m layer. y_k^m represents the output of the kth neuron in m layer, and the activation function used in 1-D CNN is defined as $f(\cdot)$.

(2) Backward-propagation

Assume that the loss function of the sample in the output layer of the network is:

$$e = \frac{1}{n} \cdot \sum_{k=1}^{n} (o_k - y_k)^2.$$
 (11)

In Eqn (11), n is the number of neurons in the output layer of the network, y_k is the output on the kth neuron, and o_k is the ideal output of the objective function. Calculate the partial derivative of the error e with respect to the weight w and the bias b respectively, and then use the gradient descent method to update. The loss function of backward- propagation, expressed in Eqn (11), minimizes the difference between the predicted compaction quality metrics and real measurements, driving the network to improve its predictions iteratively.

4.3. Simulation process adaptive adjustment

In Sections 4.1 and 4.2, we described the methods for determining construction simulation parameters and evaluating compaction quality, respectively. In this section, we will elaborate on how to adaptively adjust the construction simulation logic when the simulation clock advances to the layer CPM model. In the CPM model, after the quality inspection activity of the last rolling band is completed, it is judged whether the layer needs supplementary rolling. Steps are as follows.

(1) Simulation parameter assignment

Based on the real-time monitoring system and DPM model, the probability density distribution of VC value, air content, and rolling speed and deflection angle is obtained. Randomly assign values to each grid in the layer according to the probability distribution of VC value, air content, and rolling speed and deflection angle.

(2) Compaction degree calculation

Calculate the number of rolling passes through the simulation of the rolling process, At the same time, the compaction quality analysis model is carried out, and the compaction degree of the roller compacted concrete at each grid position is calculated.

(3) Supplementary rolling judgment

According to the formula below, the compaction quality standard ratio (r_r) of the layer is calculated:

$$r_r = N_{r,a} / N. (12)$$

In Eqn (12), $N_{r,q}$ is defined as the number of grids with qualified compaction quality, N is defined as the total number of the layer grids.

If $r_r \geq r_{r,0}$, $r_{r,0}$ is the qualified ratio of the compaction quality standard in the layer, no need for supplementary rolling, layer construction CPM model does not include supplementary rolling activity. If $r_r < r_{r,0}$, add supplementary rolling activity in the layer construction CPM model, and enter step (4) to calculate supplementary rolling duration.

(4) Supplementary rolling area priority determination

Combine adjacent unqualified grids into area (A_i) , comprehensively consider the area and compaction quality of each unqualified area, and determine the priority of the area that needs to supplementary rolling.

(5) Transition time calculation

After determining the supplementary rolling area, the path (l) of the roller from its current position to the supplementary rolling area (A_i) could be determined, then calculate the corresponding supplementary rolling transition time according to the average rolling speed (\overline{V}_r) of the storehouse surface.

(6) Calculate supplementary rolling parameter

Through the intelligent analysis model of compaction quality, the passes of static rolling and vibrating rolling is gradually increased to determine the minimum number of supplementary rolling passes.

(7) Area (A_i) supplementary rolling simulation

Randomly generate the rolling speed (v) and rolling deflection angle (θ) to simulate the process of Area (A_i) supplementary rolling, after finishing supplementary rolling, return to step (2) to calculate the compaction degree and judge whether supplementary rolling is necessary again, until the layer compaction quality is qualified.

(8) Calculation of total supplementary rolling duration.

5. Solution method based on DES and deep learning

In Section 4 of this paper, we constructed a dynamic construction progress simulation mathematical model based on the CPM network planning technique, CYCLONE simulation technology, and mathematical modeling methods. In this chapter, we will present the solution process based on the principles of discrete event simulation and deep learning methods. Concrete rolling construction could be modeled as a discrete stochastic dynamic service system. As shown in Figure 6, Global simulation clock, local sim-

ulation clock and rolling process simulation clock are respectively set to advance the storehouse surface CYCLONE model, the CPM model of simulation process of the layers and the simulation process of rolling. It can simulate the rolling process of rolling compacted concrete in the operation level and the activity level, which ensures the refinement and efficiency of the simulation process. To record the running trajectory of simulation time, the three simulation clocks use next-event time advance (Law, 2015).

In each simulation cycle, the monitoring data of concrete rolling construction is obtained firstly. The data mainly includes concrete property parameters and rolling parameter. After simulation parameter imputation and global simulation clock initialization, global simulation clock advances Δt to judge whether event has occurred. If an event occurs, the system will enter the event and determine whether it is a simulation event, while correspondingly changing the state of relevant entities in the system. Local simulation clock is invoked to simulate the layer construction at the time that global simulation clock reaches layer activity. The activity level of the rolling process is tracked by recording the roller's position, the number of passes completed over a specific area, and the compaction energy applied. These parameters are continuously updated and used to assess event triggers, such as the completion of a compaction cycle or the need for additional passes.

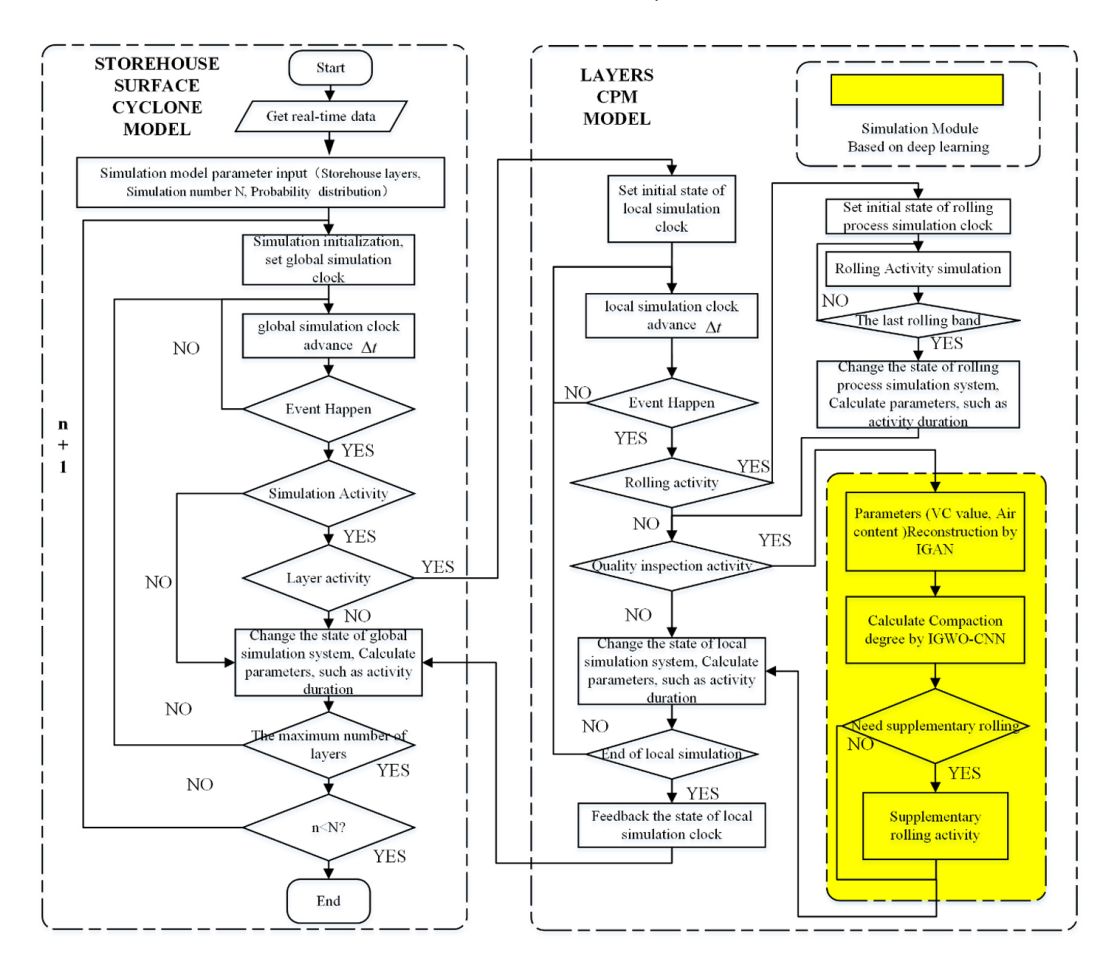


Figure 6. Model solving process based on discrete event simulation method and deep learning

When local simulation clock reaches rolling activity, the rolling process simulation clock is invoked and the concrete rolling process is simulated. Until rolling process is completed, the rolling process simulation system records the rolling duration and rolling passes of each grid. When local simulation clock reaches quality inspection activity, concrete property parameters are reconstructed by IGAN, then VC, air content, rolling speed and rolling passes are used to calculate each grid compaction degree by IWGO-CNN. If supplementary rolling is needed, the supplementary rolling is simulated.

In this paper, t-distribution method is used to solve the confidence interval of the construction duration with a confidence level of $1-\alpha$. The solution steps are as follows.

(1) Calculate the mean value of simulation duration \bar{x} and variance S^2 :

$$\overline{x} = \frac{1}{n} \sum_{i=1}^{n} \xi_{i};$$

$$S^{2} = \frac{1}{n-1} \sum_{i=1}^{n} (\xi_{i} - \overline{x})^{2} = \frac{1}{n-1} \left[\sum_{i=1}^{n} \xi_{i}^{2} - n\overline{x}^{2} \right].$$
(13)

In Eqn (13), \bar{x} is the mean value of simulation duration, ξ_i is the value of each simulation duration, S^2 is the variance of simulation duration, n the number of simulation times.

(2) Structure pivot:

$$T = \frac{\overline{x} - \mu}{\frac{s}{\sqrt{n}}} \sim t_{n-1}.$$
 (14)

(3) Shortest confidence interval

For a given a, find b and c so that the following formula:

$$P\left\{a \le T \le b\right\} = P\left\{a \le \frac{\overline{x} - \mu}{\sqrt[5]{n}} \le b\right\} = 1 - \alpha. \tag{15}$$

In Eqn (14), α is confidence, a is the lower limit of the pivot interval, b is the upper limit of the pivot interval.

When $b = -a = t_{n-1} \left(\frac{\alpha}{2}\right)$, the length of the confidence interval is the shortest.

(4) Calculate the confidence interval of the construction duration

Solve the inequality:

$$t_{n-1}\left(\frac{\alpha}{2}\right) \le \frac{\overline{x} - \mu}{\sqrt[5]{n}} \le t_{n-1}\left(\frac{\alpha}{2}\right). \tag{16}$$

The confidence interval of the construction duration with a confidence level of $1 - \alpha$ is calculated:

$$\left[\overline{x} - t_{n-1} \left(\frac{\alpha}{2}\right) \cdot \frac{S}{\sqrt{n}}, \ \overline{x} + t_{n-1} \left(\frac{\alpha}{2}\right) \cdot \frac{S}{\sqrt{n}}\right]. \tag{17}$$

6. Case study

To validate the feasibility and effectiveness of the simulation model, a roller compacted concrete dam (HD dam) located in Yunnan province, southwest China is selected as a case study.

The proposed simulation model was programmed in Python 3.7.10 and Visual Studio 2019. In addition, the deep learning module is programmed in python language, and the rest of the simulation modules are programmed in C++ language. The simulation program interface is shown in the Figure 7.

Generally, concrete rolling construction takes the storehouse as the placement unit. Taking Storehouse 10#~11#—1468 m~1471 m as an example, the adaptive adjustment analysis of the simulation process is carried out. The placement process adopts a horizonal layer organization form, and the storehouse is divided into 10 rolling layers. It is equipped with 4 paving machines and 9 rolling machines. The standard rolling pass of the storehouse surface is static rolling 2 passes plus vibrating rolling 6 passes and the design rolling speed is 2 km/h.

6.1. Rolling parameters and concrete property parameters

First, based on the real-time monitoring system of concrete rolling construction, the concrete property parameters and rolling parameters of the storehouses before the construction of the pouring storehouse 10#~11#—1468 m~1471 m are collected.

Then, according to the refined simulation process of the storehouse surface construction, the storehouse surface construction preparation activities before the first layer construction are simulated, and the simulation clock is advanced to the first layer level construction in the storehouse surface construction CYLCLONE model.

When simulating the construction of the first layer, call the layer CPM model and the rolling process simulation model in the construction simulation program until the quality inspection of the last rolling band is completed. At the same time, through the rolling process simulation in the construction simulation program, the number of static rolling passes, the number of rolling passes and the average rolling speed at each grid in the layer have been obtained. Meanwhile, samples of concrete property parameters are enriched based on IGAN.

The reconstruction result is shown in Figures 8a and 8b.

The training set has a total of 1064 data, the batch size is 64, the epochs is 100, and the training process will iterate 1600 times. The loss function curve of the training process is shown in Figure 8c. It can be seen from the figure that the discriminant loss fluctuates around zero after 50 iterations. The generation loss is stable after 1300 iterations and fluctuates around zero. To test whether underfitting of the model occurs, the Kullback-Leibler Divergence (Bishop & Nasrabadi, 2006) and RMSE of the vc and

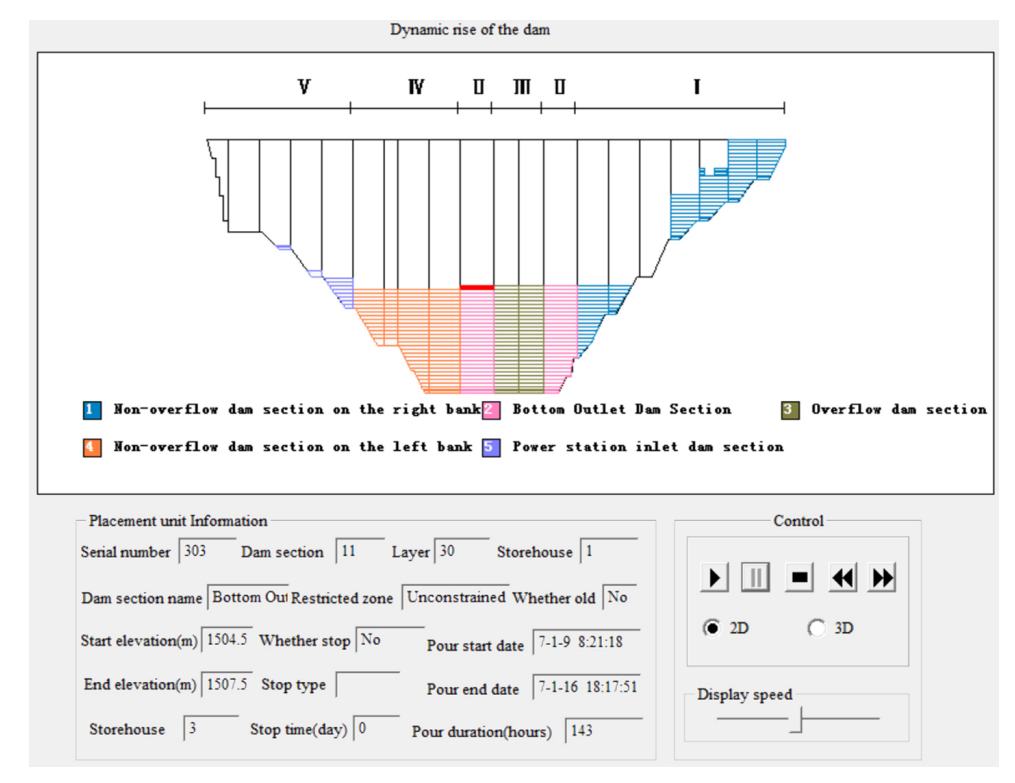


Figure 7. HD dam construction simulation program

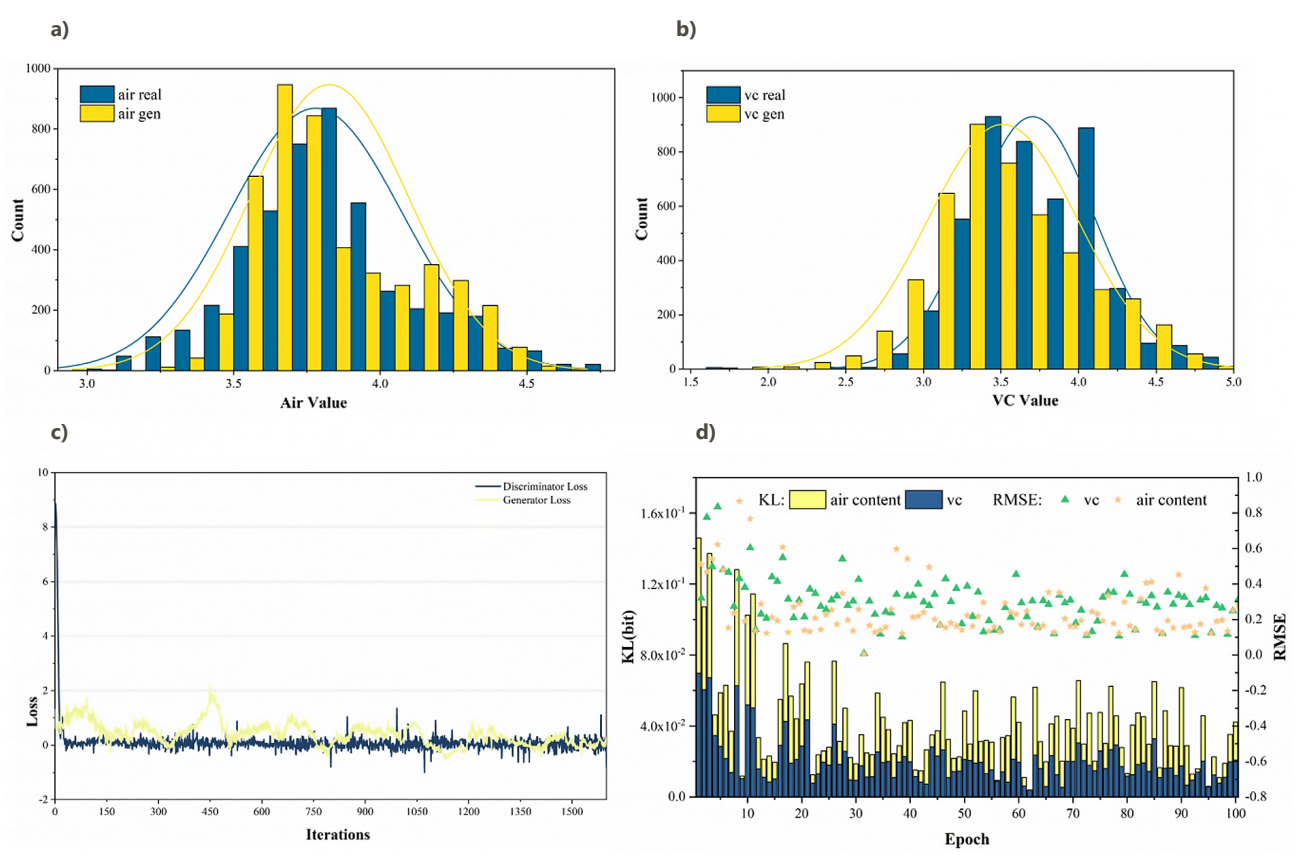


Figure 8. Concrete property parameters reconstruction result

air content generated samples and the real samples were calculated when the epoch is 100, and the Kullback-Leibler (KL) Divergence calculation formula is shown in Eqn (18):

$$D_{KL}(p \parallel q) = \sum_{i=1}^{N} p(x_i) \log \left(\frac{p(x_i)}{q(x_i)} \right). \tag{18}$$

In Eqn (18), $p(x_i)$ is true distribution, $q(x_i)$ is approximate distribution. When epoch is 100, the KL Divergence and RMSE of vc are calculated to be 0.0177 and 0.406, respectively, while the KL Divergence and RMSE of Air content are calculated to be 0.0192 and 0.377, respectively. The result shows that the model performs well on the training set. At the same time, in order to avoid overfitting, the dropout algorithm is used to randomly set the neuron activation function of a part of the hidden layer to 0 during each iteration of the training process. In order to verify the generalization ability of the model, a total of 327 pieces of data in the test set were tested. The Kullback-Leibler Divergence and RMSE of each epoch are shown in Figure 8d. We can be seen from the figure that with the increase of epoch, Kullback-Leibler Divergence and RMSE fluctuate occasionally, but the overall trend is convergence.

Finally, according to the probability density estimation method based on the DPM model, the probability density function of the reconstructed VC value is determined as

$$f(x) = 0.3214N(\mu_1, \sigma_1^2) + 0.0348N(\mu_2, \sigma_2^2) + 0.3214N(\mu_3, \sigma_3^2) + 0.2876N(\mu_4, \sigma_4^2) + 0.0348N(\mu_5, \sigma_5^2),$$
 where

$$\begin{split} &\pi\big(\mu_{1},\tau_{1}\big) = N(\mu_{1} \mid -0.031, \left(0.003\tau)^{-1}\right) Gamma\big(\tau_{1} \mid 172.00, 153.823\big); \\ &\pi\big(\mu_{2},\tau_{2}\big) = N(\mu_{2} \mid -2.202, \left(0.027\tau\right)^{-1}\big) Gamma\big(\tau_{2} \mid 19.50, 15.359\big); \\ &\pi\big(\mu_{3},\tau_{3}\big) = N(\mu_{3} \mid 0.703, \left(0.003\tau\right)^{-1}\big) Gamma\big(\tau_{3} \mid 172.00, 59.696\big); \\ &\pi\big(\mu_{4},\tau_{4}\big) = N(\mu_{4} \mid -0.638, \left(0.003\tau\right)^{-1}\big) Gamma\big(\tau_{4} \mid 154.00, 20.442\big); \\ &\pi\big(\mu_{5},\tau_{5}\big) = N(\mu_{5} \mid 1.265, \left(0.027\tau\right)^{-1}\big) Gamma\big(\tau_{5} \mid 19.50, 16.769\big), \end{split}$$

the probability density function of the reconstructed air content value is determined as:

$$\begin{split} f(x) &= 0.3214 N(\mu_1, \sigma_1^2) + 0.3139 N(\mu_2, \sigma_2^2) + \\ 0.3214 N(\mu_3, \sigma_3^2) + 0.0432 N(\mu_4, \sigma_4^2) \; , \end{split}$$

where

$$\begin{split} &\pi\left(\mu_{1},\tau_{1}\right)=\textit{N}(\mu_{1}\mid 0.110, \left(0.003\tau\right)^{-1}\right)\textit{Gamma}\left(\tau_{1}|172.00,133.31\right);\\ &\pi\left(\mu_{2},\tau_{2}\right)=\textit{N}(\mu_{2}\mid -0.828, \left(0.003\tau\right)^{-1}\right)\textit{Gamma}\left(\tau_{2}|168.00,91.383\right);\\ &\pi\left(\mu_{3},\tau_{3}\right)=\textit{N}(\mu_{3}\mid 0.508, \left(0.003\tau\right)^{-1}\right)\textit{Gamma}\left(\tau_{3}|172.00,92.652\right);\\ &\pi\left(\mu_{4},\tau_{4}\right)=\textit{N}(\mu_{4}\mid 1.417, \left(0.022\tau\right)^{-1}\right)\textit{Gamma}(\tau_{4}\mid 24.00,8.280)\;. \end{split}$$

6.2. Compaction degree calculation

Firstly, the prediction model is trained based on the existing monitoring data to obtain the optimal CNN hyperparameters. The total sample is 256 data, 70 data are randomly selected as the test set, and the others are used as the training set. Set the epochs of CNN to 100, the popsize of IGWO to 50, and the iterations of IGWO to 100 for training. After optimization, the batch size, number of kernels, and kernel size are obtained as 6, 32, 2. The test set prediction results are shown in the Figure 9a.

In order to analyze the validity and superiority of the model, as Figure 9b shows, this paper compares and analyzes the algorithm in this paper with SVR, CNN, and Random forest. By comparison, it is found that IGWO-CNN is better than other methods except that the maximum absolute error is larger than that of Random forest, and the overall evaluation performance is better. Among them, the R^2 of IGWO-CNN is 0.8596, while the R^2 values of SVR, CNN, and Random Forest are 0.779, 0.8123, and 0.8498, respectively. By examining the MAE, it can be observed that the proposed model still outperforms the other three models. The MAE of IGWO-CNN is 0.3491, which is the smallest among the four methods. The RMSE of IGWO-CNN is 0.4235, which is the smallest. Furthermore, the MSE performance of the IGWO-CNN model is also better than that of the other three models, which is 0.1794.

Then the IGWO-CNN model is called to obtain the compaction degree of the first layer after the initial rolling, as shown in Figure 10.

The calculated layer compaction quality standard ratio is 93.73%, which does not meet the qualified ratio of the compaction quality standard in the layer (95%). Supplementary rolling is needed, so the supplementary rolling activity is added after the last quality inspection activity of the CPM model. Next, calculate the duration of the supplementary rolling process. Consider the area and compaction quality of each unqualified area, and determine the priority of the area that needs to supplementary rolling.

As shown in Figure 11, the unqualified areas A_1 , A_2 , A_3 , and A_4 have larger areas and lower compaction degree, so the unqualified areas A_1 , A_2 , A_3 , and A_4 need supplementary rolling. Since the layer is equipped with 9 roller, one roller is arranged for each unqualified area.

Assuming that at the end of the first rolling of the layer, the roller are all located at the end of rolling bands. The calculated distances between the roller and the nearest end of the supplementary rolling area are 47.15 m, 6.52 m, 119.36 m and 50.99 m, respectively. At the rolling speed of 2 km/h, the transition time to A_1 , A_2 , and A_3 is 1.41 min, 0.20 min, 3.58 min and 1.53 min, respectively.

Finally, the IGWO-CNN model is called, and a trial algorithm is used to determine that at a rolling speed of 2 km/h, areas A_1 , A_2 , A_3 , and A_4 need to add vibrating rolling 1 pass plus static rolling 1 pass, vibrating rolling 1 pass, vibrating rolling 1 pass and static rolling, 2 passes respectively. According to the maximum length and maximum width of the unqualified area, the rolling process simulation was carried out, and the rolling duration of the area is 1.76 min, 1.38 min, 1.59 min, and 2.16 min, respectively.

After the simulation of the supplementary rolling process is completed, the IGWO-CNN model is called again to calculate the compaction degree of the layer, and the result is shown in Figure 11. Although area A_2 , A_3 , and A_4 still have grids that compaction degree has not reached 98%, the layer compaction quality standard ratio has reached 96.78%, and there is no need for supplementary rolling.

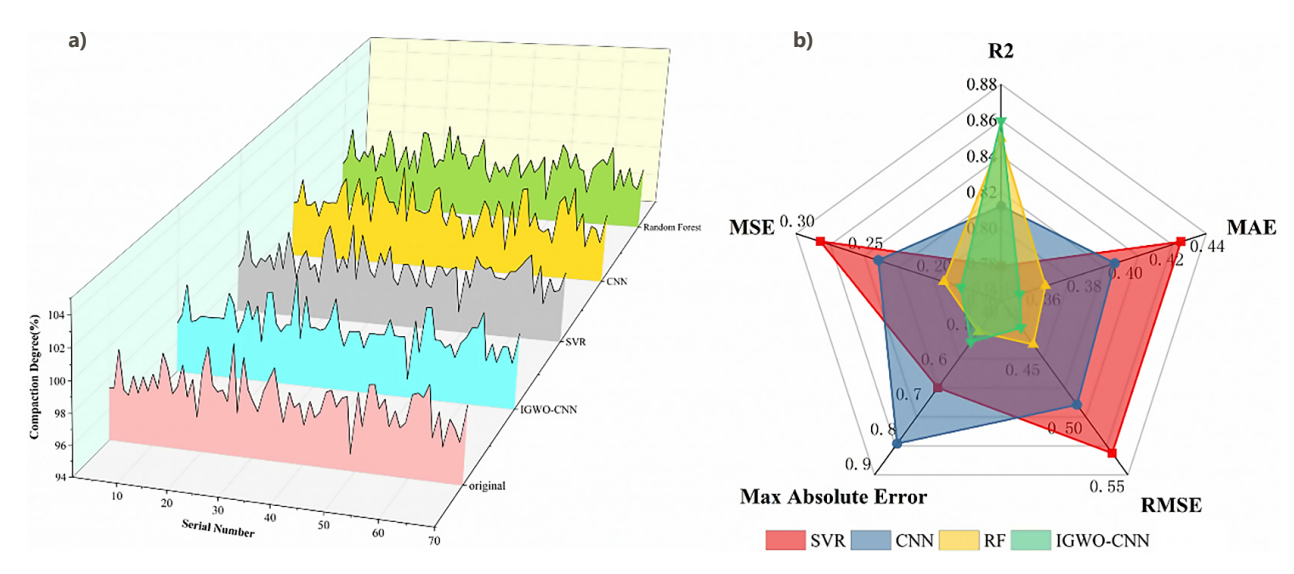


Figure 9. Compaction quality evaluation results

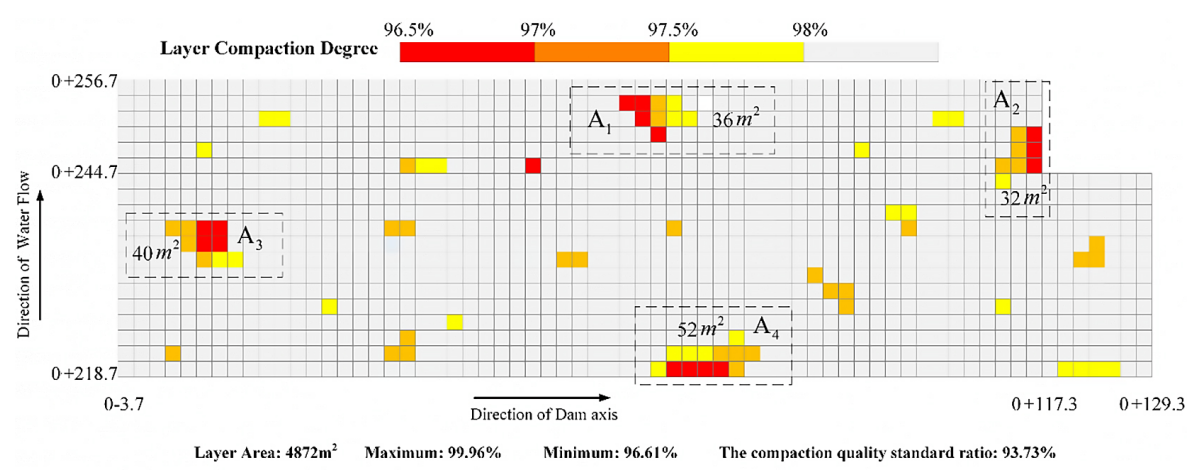


Figure 10. Layer compaction degree after initial rolling

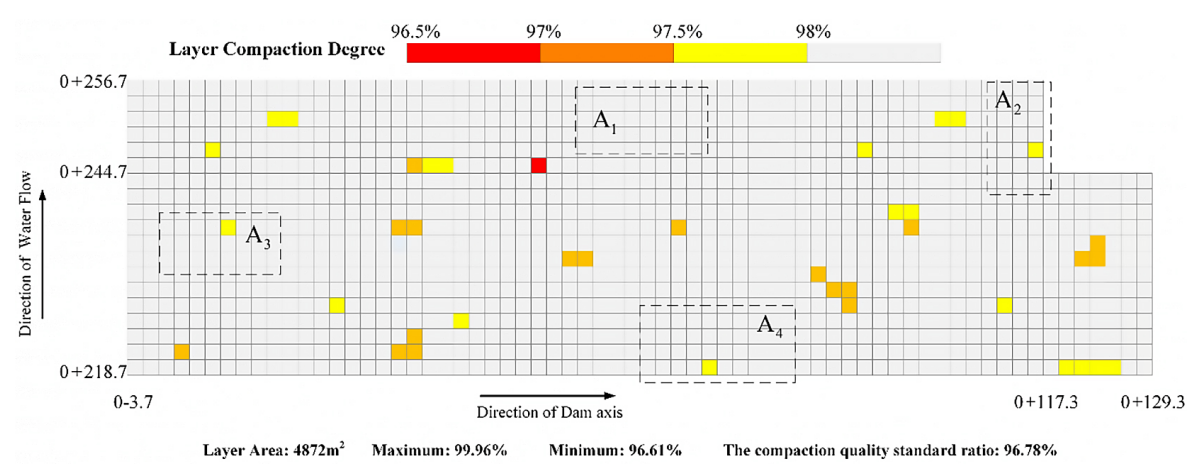


Figure 11. Layer compaction degree after supplementary rolling

Calculate the sum of the transition and rolling time of area A_1 , A_2 , A_3 , and A_4 respectively, the longest time is the supplementary rolling duration of the entire layer, so that the layer supplementary rolling duration is 5.17 min. According to the average value of each grid compaction degree, the average compaction degree of the first layer is 98.66%.

6.3. Construction simulation result

Through the above cycle, until the simulation of the last layer of the storehouse surface is completed, the supplementary rolling duration and the average value of compaction degree of each layer is obtained as shown in Table 4. Among them, the 6th and 10th layer construction simulation did not carry out supplementary rolling adjustment.

Table 4. Storehouse 10#~11#-1468 m~1471 m simulation result

Layer number	Supplementary rolling Duration (min)	Mean value of Compaction degree (%)		
1	5.17	98.66		
2	4.69	98.95		
3	7.92	98.67		
4	4.49	98.79		
5	3.90	99.17		
6	/	98.19		
7	3.29	98.46		
8	4.64	99.60		
9	4.41	98.87		
10	/	98.11		

Note: "/" means no supplementary rolling.

7. Discussion

The effectiveness of the proposed simulation model for the storehouse surface in the schedule analysis is verified by comparing the construction duration obtained by the simulation with the actual construction duration. HD dam is divided into ten construction areas, this paper takes the typical 10 storehouses in construction area 1 as an example. The construction time lasted from 15:45 on June 30, the fifth year of construction of the project to 17:26 on December 24, the fifth year of construction of the project. Excluding the interval between storehouses, the total actual construction duration of the storehouses is 798.58 hours.

In order to explore the influence of the compaction quality on the simulation accuracy, this paper conducts a refined analysis of the simulation modes 1 and 2. The details are shown in Table 5.

Simulation modes 1 represents the simulation mode without considering the compaction quality, in contrast, mode 2 considers the compaction quality. To measure the

degree of this deviation, define the deviation rate:

$$D_n = \frac{1}{n} \sum_{i=1}^{n} \frac{|T_s^i - T_a|}{T_a} \times 100\%.$$
 (19)

In Eqn (19), n is simulation times, in this simulation n = 100, T_s^i is the construction duration obtained by the ith simulation, T_a is actual construction duration, D_n is the deviation rate of construction duration after n simulations.

Based on the simulation results in Table 5, it can be found that the deviation rates of the two simulation modes show a downward trend as a whole. The reason is with the progress of the construction process, the perception of data continues to increase, the sample size of construction data continues to increase, and the estimated construction parameter distribution is closer to reality. At the same time, the deviation between the simulation construction duration and the actual construction duration is gradually reduced, which proves that the simulation accuracy has also been correspondingly improved.

Table 5 shows the simulated construction duration and actual construction duration of the typical 10 storehouses in construction area I. Except for the second storehouse in simulation mode 1 and the third storehouse in simulation mode 2, the 95% confidence interval of the simulation construction duration of all storehouses includes the actual construction duration, which proves the effectiveness of the proposed simulation of roller compacter concrete construction. Specially, the deviation rate of third storehouse in simulation mode 2 is 9.21%, it is larger than second storehouse' deviation rate which is 8.98%. Analyzing the causes of the above two phenomena, it is not difficult to find that these storehouses are in dynamic stage I, since construction area I is the first placement area of the entire roller compacter concrete dam project, construction machinery and personnel are still in the construction adaptation period, and the construction conditions of the storehouse surface change frequently. The construction conditions in the early stage of construction are unstable, so the simulation results will be biased. With the progress of the dam construction progress, the proficiency of construc-

Table 5. Typical 10 storehouses duration comparation

	Real duration (h)	Simulation duration of mode 1			Simulation duration of mode 2				
Storehouse		1.4	95% confidence intervals		D_n	Mean	95% confidence intervals		D_n
			infimum (h)	Supremum (h)	(%)	(h)	infimum (h)	Supremum (h)	(%)
1#	137.13	*	*	*	*	*	*	*	*
2#	90.36	87.13	84.87	89.39	9.86	88.66	86.64	90.68	8.98
3#	72.04	73.73	72.02	75.44	9.26	73.79	72.10	75.49	9.21
4#	68.17	69.35	67.84	70.86	8.57	68.44	67.02	69.85	8.26
5#	81.89	81.52	79.93	83.10	7.86	82.03	80.54	83.51	7.18
6#	66.51	65.45	64.27	66.64	6.90	66.92	65.78	68.06	6.85
7#	81.38	82.88	81.25	84.51	8.44	81.26	80.16	82.36	5.49
8#	58.05	58.92	57.92	59.92	7.58	58.78	57.71	59.85	7.43
9#	70.67	70.29	69.18	71.40	6.01	70.29	69.45	71.14	4.91
10#	72.38	72.29	71.24	73.34	5.89	72.86	72.30	73.43	3.22

tion operations and management continues to improve, and the overall construction conditions tend to be stable.

The above analysis shows that the simulation model considering compaction quality can improve the accuracy of construction simulation; at the same time, it also shows that by providing sufficient simulation parameters, the established refined simulation model for storehouse surface construction can accurately reflect the real construction process.

8. Conclusions and future work

Construction schedule and quality are major concerns for construction manager. This research developed a deep learning based simulation model which could analysis construction schedule and quality, Simultaneously, take concrete rolling construction as an example to verify the superiority of the model.

The contribution of this study is accurately evaluating compaction degree of the layer, which can be integrated into the RCC construction simulation program. First, the rolling process monitoring data is reconstructed by IGAN methods, and then a compaction degree analysis model based on IGWO-CNN is proposed. Finally, engineering examples are used to validate the model's simulation performance, and the results are compared to traditional simulation without considering compaction quality. The main achievements of this paper are listed as follows:

- (1) Based on the study of monitoring data of concrete property parameter, a IGAN method is used to expand the concrete performance parameter sample to provide sufficient data for the simulation parameter update.
- (2) A compaction evaluation model for dealing with complex nonlinear mapping relationships is proposed. Result shows that IGWO-CNN performs with the higher accuracy.
- (3) To simulate the project's schedule, a construction schedule simulation method based on the roller compacter concrete construction real-time monitoring system is built. The compaction degree analysis model is integrated into the roller compacted concrete construction simulation model, and it allows for an effective compaction degree analysis and a construction schedule simulation for the roller compacter concrete construction, which allows for an accurate analysis of the storehouse compaction quality and the efficient development of the construction schedule.

As far as we know, this is a good application for detailed analysis of the influence of compaction quality factors on the simulation process in the simulation of roller compacter concrete construction. In future research, some enhancements could be made in our research. On the one hand, more possible impact factors such as roller compacter concrete compaction stiffness on compaction degree could be further considered to increase the pre-

cision of the simulation model. By collecting more realtime monitoring data, we can more comprehensively analyze the impact of various factors on compaction quality and construction progress, thus improving the accuracy of compaction quality evaluation and construction progress simulation models. On the other hand, more integrated simulation models could be created to analysis the complicated relationships between multiple project performance parameters (such as cost, safety and schedule) and crucial impact variables (such as human behavior, equipment efficiency and weather). Furthermore, although the proposed simulation model can substantially enhance concrete construction quality evaluation and simulation accuracy of duration, its reliability and accuracy are heavily reliant on the availability and quality of data, so new data mining techniques should be used to improve computing efficiency.

Acknowledgements

This work is supported by the Yalong River Joint Funds of the National Natural Science Foundation of China (No. U1965207).

Author contributions

Geng Zhang: Conceptualization, Methodology, Writing – Original draft preparation, Software. Binping Wu: Review & Editing, Supervision, Validation. Bingyu Ren: Conceptualization; Validation, Investigation. Tao Guan: Methodology, Writing, Supervision. Jia Yu: Resources, Supervision, Visualization.

References

- AbouRizk, S., & Mohamed, Y. (2000). Simphony an integrated environment for construction simulation. Orlando, FL, USA. https://doi.org/10.1109/WSC.2000.899185
- Aghaeipour, A., & Madhkhan, M. (2020). Mechanical properties and durability of roller compacted concrete pavement (RCCP) a review. *Road Materials and Pavement Design*, *21*(7), 1775–1798. https://doi.org/10.1080/14680629.2019.1579754
- Akhavian, R., & Behzadan, A. H. (2015). Construction equipment activity recognition for simulation input modeling using mobile sensors and machine learning classifiers. *Advanced Engineering Informatics*, 29(4), 867–877. https://doi.org/10.1016/j.aei.2015.03.001
- Baldominos, A., Saez, Y., & Isasi, P. (2020). On the automated, evolutionary design of neural networks: Past, present, and future. *Neural Computing and Applications*, *32*(2), 519–545. https://doi.org/10.1007/s00521-019-04160-6
- Bishop, C. M., & Nasrabadi, N. M. (2006). *Pattern recognition and machine learning*. Springer.
- Celik, N., Lee, S., Vasudevan, K., & Son, Y. (2010). Dddas-based multi-fidelity simulation framework for supply chain systems. *IIE Transactions*, *42*(5), 325–341.
 - https://doi.org/10.1080/07408170903394306
- Chen, Y., Wang, Y., Kirschen, D., & Zhang, B. (2018). Model-free renewable scenario generation using generative adversarial networks. *IEEE Transactions on Power Systems*, 33(3), 3265–3275. https://doi.org/10.1109/TPWRS.2018.2794541

- Cui, C., & Fearn, T. (2018). Modern practical convolutional neural networks for multivariate regression: Applications to NIR calibration. *Chemometrics and Intelligent Laboratory Systems*, 182, 9–20. https://doi.org/10.1016/j.chemolab.2018.07.008
- Du, R., Zhong, D., Yu, J., Tong, D., & Wu, B. (2016). Construction simulation for a core rockfill dam based on optimal construction stages and zones: Case study. *Journal of Computing in Civil Engineering*, 30(3), Article 05015002. https://doi.org/10.1061/(ASCE)CP.1943-5487.0000523
- Faris, H., Aljarah, I., Al-Betar, M. A., & Mirjalili, S. (2018). Grey wolf optimizer: A review of recent variants and applications. *Neural Computing and Applications*, 30(2), 413–435. https://doi.org/10.1007/s00521-017-3272-5
- Flangan, C. (1990). *The Bresenham line-drawing algorithm*. Science Press.
- Goodfellow, I., Pouget-Abadie, J., Mirza, M., Xu, B., Warde-Farley, D., Ozair, S., Courville, A., & Bengio, Y. (2014). Generative adversarial nets. In *Proceedings of the 27th International Conference on Neural Information Processing Systems* (pp. 2672–2680). MIT Press.
- Goodfellow, I., Bengio, Y., & Courville, A. (2016). *Deep learning*. MIT Press.
- Guan, T., Zhong, D., Ren, B., Song, W., & Chu, Z. (2018). Construction simulation of high arch dams based on fuzzy Bayesian updating algorithm. *Journal of Zhejiang University*. A. Science, 19(7), 505–520. https://doi.org/10.1631/jzus.A1700372
- Gulrajani, I., Ahmed, F., Arjovsky, M., Dumoulin, V., & Courville, A. (2017). Improved training of Wasserstein GANs. Advances in Neural Information Processing Systems, 30, 5768–5778.
- Halpin, D. W. (1977). CYCLONE–A method for modelling job site process. *Journal of the Construction Division*, 103(3), 489–499. https://doi.org/10.1061/JCCEAZ.0000712
- Hong, Y., Tian, Z., & Sun, X. (2020). Dynamic evaluation for compaction quality of roller compacted concrete based on reliability metrics. *Journal of Construction Engineering and Management*, 146(10), Article 04020123. https://doi.org/10.1061/(ASCE)CO.1943-7862.0001925
- Hu, W., Jia, X., Zhu, X., Gong, H., Xue, G., & Huang, B. (2019a). Investigating key factors of intelligent compaction for asphalt paving: a comparative case study. *Construction and Building Materials*, 229, Article 116876.
- Hu, W., Zhong, D., Wu, B., & Li, Z. (2019b). Construction phase oriented dynamic simulation: Taking RCC dam placement process as an example. *Journal of Civil Engineering and Management*, 25(7), 654–672. https://doi.org/10.3846/jcem.2019.7948

https://doi.org/10.1016/j.conbuildmat.2019.116876

- Ioannou, P. G. (1990). UM-CYCLONE discrete event simulation system user's guide (UMCEE Rep. No. 89-12). Civil and Environmental Engineering Department, University of Michigan, USA.
- Ji, W., & AbouRizk, S. M. (2018). Data-driven simulation model for quality-induced rework cost estimation and control using absorbing Markov chains. *Journal of Construction Engineering* and Management, 144(8), Article 04018078. https://doi.org/10.1061/(ASCE)CO.1943-7862.0001534
- Law, A. M. (2015). Simulation modeling and analysis (5th ed.). McGraw-Hill Education.
- Liu, D., Sun, J., Zhong, D., & Song, L. (2012). Compaction quality control of earth-rock dam construction using real-time field operation data. *Journal of Construction Engineering and Management*, 138(9), 1085–1094.
 - https://doi.org/10.1061/(ASCE)CO.1943-7862.0000510
- Liu, D., Li, Z., & Liu, J. (2015a). Experimental study on real-time control of roller compacted concrete dam compaction quality using unit compaction energy indices. Construction and Build-

- *ing Materials*, 96, 567–575. https://doi.org/10.1016/j.conbuildmat.2015.08.048
- Liu, Y., Zhong, D., Cui, B., Zhong, G., & Wei, Y. (2015b). Study on real-time construction quality monitoring of storehouse surfaces for RCC dams. *Automation in Construction*, 49(Part A), 100–112. https://doi.org/10.1016/j.autcon.2014.10.003
- Lu, M. (2003). Simplified discrete-event simulation approach for construction simulation. *Journal of Construction Engineering* and Management, 129(5), 537–546. https://doi.org/10.1061/(ASCE)0733-9364(2003)129:5(537)
- Luo, W., Liu, Q., & Hu, Z. (2009). Study on RCC dam construction system coupling based on Petri net. *Journal of System Simulation*, *21*(7), 2053–2056 (in Chinese).
- Lv, F., Wang, J., Cui, B., Yu, J., Sun, J., & Zhang, J. (2020). An improved extreme gradient boosting approach to vehicle speed prediction for construction simulation of earthwork. *Automation in Construction*, 119, Article 103351. https://doi.org/10.1016/j.autcon.2020.103351
- Martinez, J. C., & Ioannou P. G. (1994). General purpose simulation with stroboscope. In *Proceedings of Winter Simulation Conference* (pp. 1159–1166). IEEE. https://doi.org/10.1109/WSC.1994.717503
- Mohamed, E., Jafari, P., & Siu, M. F. F. (2017). Data-driven simulation-based model for planning roadway operation and maintenance projects. In *Proceedings of 2017 Winter Simulation Conference* (pp. 3323–3333). IEEE. https://doi.org/10.1109/WSC.2017.8248049
- National Energy Administration of People's Republic of China. (2009). Construction specifications for hydraulic RCC (DL/T5112-2009). Water Power Press (in Chinese).
- Oloufa, A. A. (1993). Modeling operational activities in object-oriented simulation. *Journal of Computing in Civil Engineering*, 7(1), 94–106. https://doi.org/10.1061/(ASCE)0887-3801(1993)7:1(94)
- Panahi, M., Sadhasivam, N., Pourghasemi, H. R., Rezaie, F., & Lee, S. (2020). Spatial prediction of groundwater potential mapping based on convolutional neural network (CNN) and support vector regression (SVR). *Journal of Hydrology*, 588, Article 125033. https://doi.org/10.1016/j.jhydrol.2020.125033
- Shrestha, P., & Behzadan, A. H. (2018). Chaos theory-inspired evolutionary method to refine imperfect sensor data for data-driven construction simulation. *Journal of Construction Engineering and Management*, 144(3), Article 04018001. https://doi.org/10.1061/(ASCE)CO.1943-7862.0001441
- Song, L., & Eldin, N. N. (2012). Adaptive real-time tracking and simulation of heavy construction operations for look-ahead scheduling. *Automation in Construction*, 27, 32–39. https://doi.org/10.1016/j.autcon.2012.05.007
- Song, W., Guan, T., Ren, B., Yu, J., Wang, J., & Wu, B. (2020). Real-time construction simulation coupling a concrete temperature field interval prediction model with optimized hybrid-kernel RVM for arch dams. *Energies*, 13(17), Article 4487. https://doi.org/10.3390/en13174487
- Vahdatikhaki, F., & Hammad, A. (2014). Framework for near real-time simulation of earthmoving projects using location tracking technologies. *Automation in Construction*, 42, 50–67. https://doi.org/10.1016/j.autcon.2014.02.018
- Wang, R., Zhong, D., & Zha, J. (1995). Simulation study on the construction process of high roller compacted concrete dam. *Journal of Hydroelectric Engineering*, 1, 25–37 (in Chinese).
- Wang, H., Li, G., Wang, G., Peng, J., Jiang, H., & Liu, Y. (2017). Deep learning based ensemble approach for probabilistic wind power forecasting. *Applied Energy*, 188, 56–70. https://doi.org/10.1016/j.apenergy.2016.11.111

- Wang, J., Zhong, D., Adeli, H., Wang, D., Liu, M. (2018a). Smart bacteria-foraging algorithm-based customized kernel support vector regression and enhanced probabilistic neural network for compaction quality assessment and control of earth-rock dam. *Expert Systems*, 35(6), Article e12357. https://doi.org/10.1111/exsy.12357
- Wang, Q., Zhong, D., Wu, B., Yu, J., & Chang, H. (2018b). Construction simulation approach of roller-compacted concrete dam based on real-time monitoring. *Journal of Zhejiang University*. A. Science, 19(5), 367–383. https://doi.org/10.1631/jzus.A1700042
- Xu, Y., Li, F., & Asgari, A. (2022). Prediction and optimization of heating and cooling loads in a residential building based on multi-layer perceptron neural network and different optimization algorithms. *Energy*, 240, Article 122692. https://doi.org/10.1016/j.energy.2021.122692
- Zhang, S., Du, C., Sa, W., Wang, C., & Wang, G. (2014). Bayesian-based hybrid simulation approach to project completion fore-casting for underground construction. *Journal of Construction Engineering and Management 140*(1), Article 04013031. https://doi.org/10.1061/(ASCE)CO.1943-7862.0000764
- Zhang, J., & Zeng, D. (2018). Experimental research on construction technology of roller compacted concrete. *China Water Transport*, *18*(9), 257–258 (in Chinese).
- Zhang, J., Yu, J., Guan, T., Wang, J., Tong, D., & Wu, B. (2020). Adaptive compaction construction simulation based on Bayesian field theory. *Sensors*, 20(18), Article 5178. https://doi.org/10.3390/s20185178
- Zhang, Y., Zhou, B., Cai, X., Guo, W., Ding, X., & Yuan, X. (2021). Missing value imputation in multivariate time series with end-to-end generative adversarial networks. *Information Sciences*, 551, 67–82. https://doi.org/10.1016/j.ins.2020.11.035
- Zhang, H., Zhang, W., Meng, Y., & Li, H. (2022). Deterioration of sea sand roller compacted concrete used in island reef airport runway under salt spray. *Construction and Building Materials*, 322, Article 126523.
 - https://doi.org/10.1016/j.conbuildmat.2022.126523
- Zhang, J., Yu, J., Yu, P., Wang, X., Tong, D., & Wang, J. (2023). Enhanced semi-supervised ensemble machine learning approach for earthwork construction simulation activity sequence automatically updating driven by weather data. *Geological Journal*, 58(6), 2231–2253. https://doi.org/10.1002/gj.4631
- Zhao, C., Dong, H., & Zhou, Y. (2013). Study on simulation and optimization of concrete placement system on construction surface of RCC dam. *Water Resources and Hydropower Engineering*, 44(1), 79–82 (in Chinese).
- Zhong, D., Hu, W., Wu, B., Li, Z., & Zhang, J. (2017). Dynamic time-cost-quality tradeoff of rockfill dam construction based on real-time monitoring. *Journal of Zhejiang University. A. Science*, *18*(1), 1–19. https://doi.org/10.1631/jzus.A1600564
- Zhong, D., Yang, S., Chang, H., Yu, J., Yan, F. (2015). Construction schedule risk analysis of high roller-compacted concrete dams based on improved CSRAM. Science China Technological Sciences, 58(6), 1021–1030.
 - https://doi.org/10.1007/s11431-015-5781-8